Atmospheric breakdown kinetics and air quality impact of potential "green" solvents the oxymethylene ethers OME3 and OME4

James D'Souza Metcalf[1,2], Ruth K. Winkless[1], Caterina Mapelli[1,2,3], C. Rob McElroy[2,4], Claudiu Roman[5,6], Cecilia Arsene[5,6,7], Romeo I. Olariu[5,6,7], Iustinian G. Bejan[5,7] and Terry J. Dillon[1].

[1]Wolfson Atmospheric Chemistry Laboratories, Department of Chemistry, University of York, York, YO10 5DD, UK.
[2]Green Chemistry Centre of Excellence, Department of Chemistry, University of York, York, YO10 5DD, UK
[3]now at: National Reasearch Council - Institute of Methodologies for Environmental Analysis (IMAA), Tito Scalo, Potenza, 85050, Italy
[4]now at: Department of Chemistry, School of Natural Sciences, University of Lincoln, Brayford Pool, Lincoln, LN6 7TS, UK
[5]Faculty of Chemistry, "Alexandru Ioan Cuza" University of Iasi, 700506, Iasi, Romania
[6]Research Center with Integrated Techniques for Atmospheric Aerosol Investigation in Romania (RECENT-AIR), "Alexandru Ioan Cuza" University of Iasi, 11th Carol I, Iasi, 700506, Romania
[7]Integrated Center of Environmental Science Studies in the North Eastern Region – CERNESIM, "Alexandru Ioan Cuza" University of Iasi, 700506, Iasi, Romania

Correspondence to: Terry J. Dillon (terry.dillon@york.ac.uk) and Iustinian G. Bejan (iustinian.bejan@uaic.ro)

Abstract. Laboratory-based experiments were used to investigate the atmospheric degradation chemistry of two oxymethylene ethers, $CH_3O(CH_2O)_3CH_3$ (OME3) and $CH_3O(CH_2O)_4CH_3$ (OME4). OME3 and OME4 have been proposed as promising "green" replacement compounds for problematic ethereal solvents such as 1,4-dioxane and tetrahydrofuran. Results from direct, absolute laser-based experiments and from a series of complementary relative rate studies demonstrated that OH + OME3 proceeded with a rate coefficient $k_3(296 \pm 2$ K$) = (1.0 \pm 0.2) \times 10^{-11}$ cm^3 molecule^{-1} s^{-1}, a factor of two smaller than predicted by structure activity relationships (SAR). Evidence for a complex mechanism was provided by $k_3(294 - 464$ K$)$, characterised by deviations from Arrhenius-like behaviour close to room temperature. A further series of relative rate experiments were used to determine a rate coefficient of $k_4(296 \pm 2$ K$)= (1.1 \pm 0.4) \times 10^{-11}$ cm^3 molecule^{-1} s^{-1} for OH + OME4. These results allowed for lifetimes, $\tau \approx 1$ day to be estimated for the removal of each of OME3 and OME4 from the troposphere. Photochemical Ozone Creation Potential estimates ($POCP_E$) were calculated for NW-Europe conditions. These were considerably smaller than equivalent metrics for the problematic solvents they may replace, largely owing to their lack of C-C bonds. In the course of this work, rate coefficients (in 10^{-11} cm^3 molecule^{-1} s^{-1}) were determined for Cl + OME3, $k_6(296 \pm 2$ K$) = (17 \pm 4)$ and for Cl + OME4, $k_7(296 \pm 2$ K$) = (19 \pm 6)$.

1   Introduction

As traditional sources of volatile organic compound (VOC) emissions are subject to increasingly strict regulation, new and formerly overlooked emission routes are growing in significance. Of these, solvents are emerging as the dominant anthropogenic source of non-methane VOC (Lewis et al., 2020). Simultaneously, the landscape of solvent use and emission

is undergoing a shift as research and industry move away from harmful and environmentally damaging petroleum derived solvents and in their place safer, renewable bio-based alternatives are being developed as part of the move towards net zero (Ashcroft et al., 2015; Bryan et al., 2018; Constable et al., 2007). While fundamental air quality metrics are discussed in some solvent selection guides and development protocols, there remains a significant and troubling lack of knowledge surrounding the atmospheric fate of newly developed "green" solvents.

The oxidative breakdown of VOC in air is known to yield harmful ozone (O_3), formaldehyde (HCHO), and particulates (Bloss et al., 2005; Hansen et al., 1975; Saunders et al., 2003). Waste and inefficient use of volatile solvents is therefore a well-established source of harmful emissions to the atmosphere. Poor air quality has been estimated to cause of over 400,000 annual deaths in Europe alone (European Environment Agency., 2020; Lelieveld et al., 2019). Ethers form a significant portion of atmospheric non-methane VOCs, and are emitted almost entirely from anthropogenic sources (Calvert et al., 2015). Whilst unsaturated ethers are known to be significantly more reactive than saturated ethers, the latter are far more widely used in solvent applications (Zhou et al., 2006). Many ethereal solvents, examples of which include 1,4-dioxane (1,4-dioxacyclohexane, $C_4H_8O_2$, henceforth dioxane) and tetrahydrofuran (oxolane, C_4H_8O, henceforth THF) are manufactured from unsustainable petrochemical feedstocks, harmful to health (potentially carcinogenic), form dangerous peroxides and are environmentally hazardous (Prat et al., 2016). Despite this, analysis of trends in solvent usage have shown that dioxane and THF consistently remain among the most widely used solvents in newly reported processes (Ashcroft et al., 2015; Jordan et al., 2021). Considerable research effort has therefore been directed towards developing sustainable and safe new "green" solvents (de Gonzalo et al., 2019; Jordan et al., 2022). Oxymethylene ethers ($CH_3O(CH_2O)nCH_3$, henceforth OME, specific ethers an OMEn) can be synthesised at scale from readily available, renewable and bio-derivable methanol (CH_3OH) and formaldehyde (HCHO) (Peter et al., 2018). With carbon capture and utilisation, circular CO_2 derived "e-methanol" is also a potential commercially available large-scale feedstock. Formaldehyde from CO_2 is also being extensively researched (Zhao et al., 2022). Numerous studies have shown that OME blends are viable as carbon neutral diesel alternatives, associated with low particulate generation due to their lack of carbon-carbon bonds (Fenard and Vanhove, 2021; Härtl et al., 2017; Jacob and Maus, 2017; Schmitz et al., 2022; Sun et al., 2025; Zhang et al., 2014). OME have also been demonstrated as safer, bio-based alternatives to traditional ethereal solvents (Zhenova et al., 2019).

A crucial, often rate-determining step in atmospheric VOC oxidation mechanisms is the initial breaking of a C-C or C-H bond, either directly *via* photolysis or following attack by oxidants such as O_3 or gas-phase free-radicals (Seinfeld, 2016). Dioxane, THF and the OME are all saturated VOC and lack a near-UV chromophore. As such their principal breakdown route is likely *via* bimolecular reaction with the principal gas-phase oxidant, the hydroxyl radical (OH), all of which likely proceed *via* H abstraction to an organic radical fragment + H_2O, e.g. (R1 – R4):

$$OH + \text{dioxane} \rightarrow \text{(products)} \qquad\qquad (R1)$$

$$OH + \text{THF} \rightarrow \text{(products)} \qquad\qquad (R2)$$

$$OH + OME3 \rightarrow \text{(products)} \qquad\qquad (R3)$$

$$OH + OME4 \rightarrow \text{(products)} \qquad\qquad (R4)$$

Rate coefficients, k(298 K) for OH-mediated removal of traditional volatile solvents are reasonably well established. The available literature for k_1 (Dagaut et al., 1990; Maurer et al., 1999; Porter et al., 1997) was most recently supplemented by Moriarty et al (2003) who estimated a lifetime $\tau_1 \approx 25$ hours for removal of dioxane from the troposphere. Literature for k_2 (Illés et al., 2021; Ravishankara and Davis, 1978; Wallington et al., 1988; Winer et al., 1977) is in agreement on a more rapid removal process for THF, for which Moriarty et al (2003) estimated $\tau_2 \approx 16$ hours. By contrast with these more established solvents, there appears to be no gas-phase data on (R3 – R4), from which to estimate lifetimes and other air quality metrics. In the absence of such data, even a cursory assessment of the environmental impact of replacing dioxane or THF with OME is not feasible. In the absence of experimental data, k-values may be predicted by Structure Activity Relationships (SAR) such as those most recently formulated by Jenkin et al. (2018). However, the lack of literature data available for OH + ethers results in SAR predictions with a large associated uncertainty. For example, we have recently reported that the atmospheric breakdown of the new "green" solvent 2,2,5,5-tetramethyloxolane (TMO) proceeds a factor of three slower than SAR prediction (Mapelli et al., 2022).

$$\text{OH} + \text{TMO} \rightarrow \text{(products)} \hspace{4cm} \text{(R5)}$$
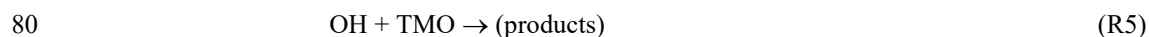
Accordingly, the objectives of this work were to use laboratory-based experiments to determine accurate values of $k3$ and $k4$ and to interpret these results in terms of atmospheric lifetimes and impacts on air quality. In the course of this work, rate coefficients were determined for reactions (R6-R7) of OME with another atmospheric oxidant, atomic chlorine. These provide a further insight into the atmospheric fate of OMEs in regions where chlorine is significant (Ariya, 1999; Atkinson and Aschmann, 1985; Thornton et al., 2010).

$$\text{Cl} + \text{OME3} \rightarrow \text{(products)} \hspace{4cm} \text{(R6)}$$
$$\text{Cl} + \text{OME4} \rightarrow \text{(products)} \hspace{4cm} \text{(R7)}$$

2 Experimental

Laboratory-based experiments were carried out using two well-established kinetic techniques. Following a description of the isolation and characterisation of OME samples in section 2.1, section 2.2 describes the Environmental Simulation Chamber made from Quartz, Universitatea Alexandru Ioan Cuza din Iaşi (ESC-Q-UAIC) facility at Alexandru Ioan Cuza University of Iasi, Romania, used for relative rate determinations of k_3(296 ± 2 K) and k_4(296 ± 2 K). The pulsed laser photolysis (PLP) apparatus used for direct, absolute determinations of k_3(294 – 464 K) at the University of York, UK, is described in section 2.3. Computational procedures used to estimate structural, spectral and kinetic parameters are outlined in section 2.4.

2.1 OME Separation and Characterisation

OME3 (2,4,6,8-tetraoxanonane) and OME4 (2,4,6,8,10-Pentaoxaundecane) were isolated from an OME blended fuel mix (ChemCom Industries) by vacuum distillation. Fractions were identified by NMR and Atmospheric Pressure Chemical Ionisation Mass Spectrometry (APCI-MS) analysis, with sample purities of > 97% estimated *via* GC-FID. OME5

(2,4,6,8,10,12-hexaoxatridecane) was similarly isolated and identified, but its vapour pressure was too low to be of utility in this work. Spectra and chromatograms of isolated fractions are contained in the supplementary information (S1).
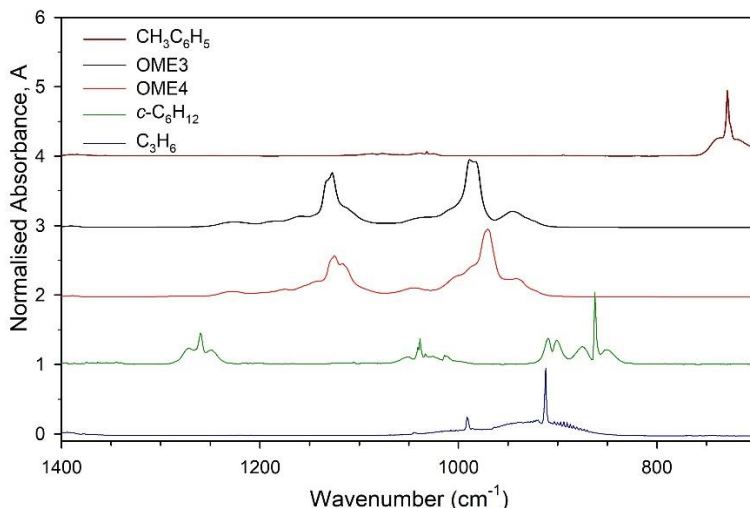
2.2   Smog Chamber Studies

Figure 1: Spectra of OME3, OME4 and reference compounds taken in ESC-Q-UAIC chamber. Compounds were monitored at, 912 cm^{-1} (C_3H_6), 862 cm^{-1} (c-C_6H_{12}), 729 cm^{-1} ($CH_3C_6H_5$) and 1128 and 989 cm^{-1} (OME3) and 1125 and 971 cm^{-1} (OME4).

Relative rate experiments were conducted in a 760 dm^3 quartz chamber, equipped with inlet ports, sampling lines, two sets of UV lamps (254 and 365 nm), and multi-pass FTIR instrumentation for monitoring of precursors, OME, reference VOC and oxidation products as described in recent publications (Roman et al., 2022). Liquid samples were supplied to the reactor by direct injection through a septum: H_2O_2 (35% in H_2O, Sigma-Aldrich); OME3 and OME4 (see section 2.1); $CH_3C_6H_5$ 99.5% (Carl Roth), c-C_6H_{12} 99.5% (Sigma-Aldrich), C_3H_6 >99.9% (Sigma-Aldrich) and $(COCl)_2$ 98% (Sigma-Aldrich) were used as supplied. A flow of air or nitrogen was used to convey the injected liquid through the heated inlet port and to avoid any loss of injected compounds on addition line. All experiments were conducted at $p = (1000 \pm 10)$ mbar (air) and $T = (296 \pm 2)$ K. OH was generated *via* the direct 254 nm photolysis of H_2O_2 (R8).

$$H_2O_2 + h\nu \rightarrow 2OH \qquad\qquad\qquad\qquad (R8)$$

For all $k_{6\text{-}7}$ determinations, atomic chlorine was generated by the photolysis of oxalyl chloride at 254 nm (R9) (Stuhr et al., 2024).

$$(COCl)_2 + h\nu \rightarrow\rightarrow 2Cl + 2CO \qquad\qquad\qquad\qquad (R9)$$

 Experiments conducted in the absence of radical precursors demonstrated that neither OME3 nor the various reference compounds were significantly impacted by wall losses or photolytic removal, indicating that only small corrections to subsequent kinetic data were necessary. Corrections were required (up to 20%) when processing OME4 data. These

4

corrections were applied in the manner we have previously reported (Mairean et al., 2024). A subtraction procedure using the FTIR software was performed at specific spectral features subtracting reference spectrum from sample spectrum and adjusting the peak intensity by a scaling factor. The obtained factors are directly proportional to species concentrations and were used to calculate the logarithmic depletion for ratio of OME and the reference compounds. According to Eq. (1), the slope obtained from a proportional fit may be identified with the relative rate k_3 / k_{ref}.

$$ln\left(\frac{[OMEn]_{t0}}{[OMEn]_t}\right) - (k_{photo} + k_{wall})(t - t_0) = \left(\frac{k_3}{k_{ref}}\right) ln\left(\frac{[reference]_{t0}}{[reference]_t}\right) \quad (1)$$

Where k_{photo} and k_{wall} are photolysis frequency (J) and rate of wall loss respectively, measured under experimental conditions for OME4 and assumed to be zero for all other compounds.

Reference compounds were selected to satisfy two main criteria. Firstly, it was desirable for the FTIR spectra of references to have well defined peaks that were close to, but overlapped minimally with, those of the OME (Fig. 1). This was achieved by comparing reference spectra to OME spectra predicted *via* DFT calculations (section 2.4). Secondly, reference compound $k(296 \pm 2$ K) data needed to be well-established in the literature (see Table 1); these values were preferably of a similar magnitude to measured or predicted target k-values. According to these principles the selected reference compounds were toluene ($CH_3C_6H_5$), propene (C_3H_6) and cyclohexane (c-C_6H_{12}), as represented in Table 1.

Table 1: Eurochamp recommended kinetic data (McGillen et al., 2020) for reference compounds used in rate coefficient determination in this work.

Reaction	Reference Reaction	k_{298} / 10^{-12} cm^3 molecule^{-1} s^{-1}	Source of recommended values
(R10)	C_3H_6 + OH	24.4 ± 3.66	"*Fitted or manually entered data from multiple sources*" (McGillen et al., 2020)
(R11)	c-C_6H_{12} + OH	6.69 ± 0.67	"*Fitted or manually entered data from multiple sources*" (McGillen et al., 2020)
(R12)	$CH_3C_6H_5$ + OH	5.60 ± 1.46	Evaluated kinetic and photochemical data for atmospheric chemistry (IUPAC) (Mellouki et al., 2021)
(R13)	C_3H_6 + Cl	270 ± 30.0	Evaluated kinetic and photochemical data for atmospheric chemistry (IUPAC) (Atkinson et al., 2006)
(R14)	c-C_6H_{12} + Cl	330 ± 49.5	(Calvert et al., 2015)
(R15)	$CH_3C_6H_5$ + Cl	60.0 ± 6.00	(Calvert et al., 2015)

Rate coefficients were taken from the EUROCHAMP Database for the Kinetics of the Gas-Phase Atmospheric Reactions of Organic Compounds version 3.1.0. (McGillen et al., 2020). FTIR spectra were recorded every minute by combining 114 scans for a spectrum, with approximately 30 such spectra at a resolution of 1 cm^{-1} completing each experiment.

2.3 PLP-LIF Experiments

Absolute determinations of k_3(294 – 502 K) were carried out in York using the PLP apparatus, detailed in recent publications (Mapelli et al., 2022, 2023). Briefly, output from a Nd:YAG laser (Quantel, Q-Smart, 20 mJ / 266 nm pulse at 10 Hz) was directed into a 400 cm3 pyrex reactor and used to generate OH *via* H_2O_2 photolysis (R8). Output from a frequency-doubled dye laser (Radiant dyes, Rhodamine-6G) was used to pump the Q11 transition of OH at 281.997 nm. Off-resonant 308 nm fluorescence was collected by a photomultiplier (Hamamatsu) to effect LIF detection of OH. Reactor temperature was regulated by heating tape and monitored by a thermocouple. Four calibrated mass flow controllers regulated gas flow rates with pressure monitored by a calibrated capacitance manometer. Such absolute rate coefficient determinations relied upon accurate knowledge of [OME]. In the case of OME3, mixtures were prepared on a vacuum line by mixing solvent vapours $\approx$ 0.5% in 1300 mbar N_2 for storage in 12 dm^3 pyrex bulbs. [OME3] values were calculated to ± 15% estimated precision from manometric measurements. Data conducted at [OME3] = 0, together with manometric estimates indicated that $[H_2O_2] \lesssim 2 \times 10^{14}$ molecules cm^{-3} and consequently that [OH] $\approx 5 \times 10^{11}$ molecule cm^{-3} was generated (R8) in each experiment. Pseudo first-order conditions, [OME3] >> [OH] and / or $[H_2O_2]$ >> [OH] therefore applied throughout.

Handling of OME4 was more of a challenge. A vapour pressure of p_{vap} = (0.62 ± 0.15) mbar was measured in a series of experiments conducted on the vacuum line at T = 296 K. OME4 volatility was consequently too low for reliable preparation and delivery *via* pyrex bulbs. OME4 was therefore supplied *via* flow of N_2 through a pyrex bubbler located upstream of the reactor. Modest flow rates of 0 - 30 sccm (N_2) were used to best aid saturation of [OME4] as the bubbler conditions were maintained at p $\approx$ 100 mbar and (with use of a thermostatic water bath) T = 296 K.

Chemicals: N_2 > 99.9999%, obtained from liquid nitrogen boil-off and O_2 (99.995%, BOC) were used as supplied; H_2O_2 (JT Baker, 60% in H_2O) was pre-concentrated by continuous flow of N_2 to remove H_2O then supplied *via* a bubbler; OME3 was isolated from other OME fractions (see section 2.1) then subjected to repeat T = 77 K freeze-pump-thaw cycles to remove air prior to dilution in N_2 and storage.

2.4 Calculations

Gaussian Calculations: IR spectrum prediction was performed using Gaussian 16 (Frisch et al., 2016), from an input created with Gaussview (version 6.1.1, Semichem). For each molecule an optimisation and frequency calculation was performed at the B3LYP level using a 6-31G basis set. IR spectra were generated in Gaussview from the predicted vibrational energies of the molecule in the Gaussian output file. Estimated spectra are included in the supplementary information (S3).

COSMO-RS calculations: Chem3D (version 21.0.0, PerkinElmer) was used to generate approximate coordinates of compounds. Energy minimisation on these structures was carried out using the inbuilt MM2 calculation tool to a minimum RMS gradient of 0.010. These minimised structures were then transferred to COSMOconf (Version 4.0, COSMOlogic GmbH & Co. KG) as .mol files. Confirmation and energy calculations were then carried out using the BP-TZVP-GAS template. The .cosmo and .energy files were transferred to COSMOthermX (Eckert and Klamt, 2016) and rate coefficients

were estimated using a local MOPAC7 implementation (MOOH) derived from that previously described by Klamt (Klamt, 1993, 1996), *via* the environmental properties menu. A comparison between COSMO-RS estimations for oxygenated VOC and the IUPAC recommended values are provided in the supporting information (S4)

Details of included files from both Gaussian and COSMO-RS calculations and the files themselves are also provided in the supplementary information (S5a and S5b respectively).

3   Results and Discussion

Results from two experimental studies are described below. In section 3.1, the results from ambient temperature relative-rate experiments are presented. Details of complementary determinations of $k_3(294 - 464$ K) in direct, absolute laser-based experiments are presented in section 3.2. Section 3.3 describes results from relative rate determinations of k_5 and k_6 (reactions of OME with Cl-atoms). The discussion section 3.4 attempts to rationalise these results in the context of predictions from structure activity relationships and the limited literature dataset for similar oxygenated VOC. Uncertainties (±) quoted throughout this work are two sigma statistical only, derived from regression analysis, unless specifically stated otherwise. In the case of relative determinations quoted uncertainties also account for the reported uncertainty in the reference rate constant, by the method we have previously described (Mairean et al., 2024).
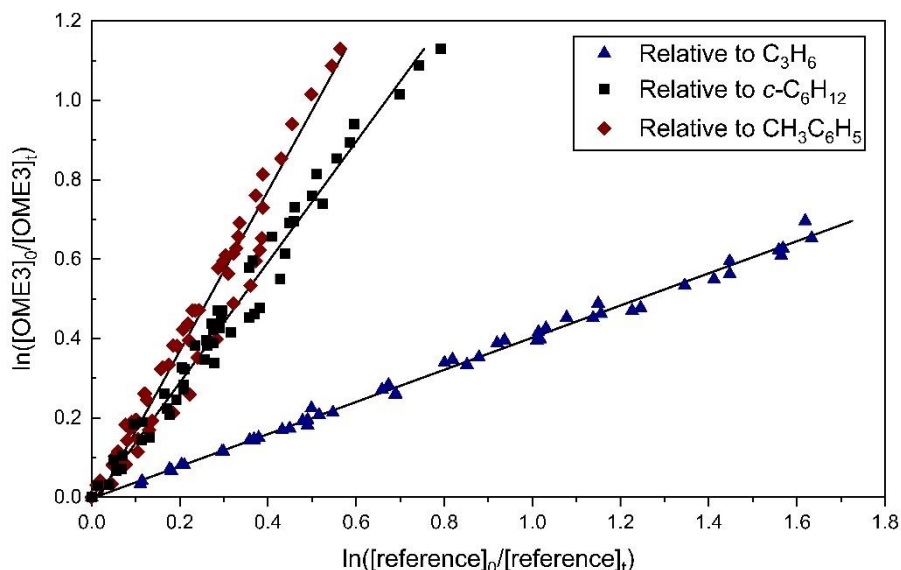
3.1   Relative Rate Determination of $k(296 \pm 2$ K)

Figure 2: Representative plot, used for relative rate determination of k_3, $k_{3RR}(296 \pm 2$ K) for OH + OME3. Blue triangles correspond to use of C_3H_6 (R10) as reference; the black squares c-C_6H_{12} (R11) and the red diamonds $CH_3C_6H_5$ (R12). The solid

190 **lines are linear fits, the gradients of which were used to obtain k_3 (Eq.3) in conjunction with literature data (Table 1). Each experiment was repeated twice, and the resulting values of k_3 (Table 2) were averaged to obtain $k_{3,RR}(296 \pm 2$ K$) = (1.04 \pm 0.09) \times 10^{-11}$ cm^3 molecule^{-1} s^{-1}.**

Figure 2 displays the results of studies using propene (C_3H_6), cyclohexane (c-C_6H_{12}) and toluene ($CH_3C_6H_5$) as reference compounds to determine $k_3(296 \pm 2$ K$)$. These data demonstrate good linearity across a wide range of relative reactant

195 concentrations. Two experiments were carried out per reference compound for both OME3 and OME4, the results of which are presented in Table 2. The spread of values appears reasonable given both the systematic uncertainties in the various literature reference rate coefficients and statistical uncertainties. Weighted mean values from all relative rate determinations were $k_{3,RR}(296 \pm 2$ K$) = (1.04 \pm 0.09) \times 10^{-11}$ cm^3 molecule^{-1} s^{-1} and $k_{4,RR}(296 \pm 2$ K$) = (1.11 \pm 0.10) \times 10^{-11}$ cm^3 molecule^{-1} s^{-1}.

200 **Table 2: Results of relative determinations of $k_3(296$ K$)$, $k_4(296$ K$)$, $k_6(296$ K$)$ and $k_7(296$ K$)$ for each reference compound.**

Reaction	Reference	k / k_{ref}	$k(296 \pm 2$ K$)$ 10^{-11} cm^3 molecule^{-1} s^{-1}
R3	$C_3H_6 + OH$ (R10)	0.40 ± 0.005	0.98 ± 0.15
R3	c-$C_6H_{12} + OH$ (R11)	1.61 ± 0.037	1.08 ± 0.11
R3	$CH_3C_6H_5 + OH$ (R12)	1.96 ± 0.032	1.10 ± 0.29
R4	$C_3H_6 + OH$ (R10)	0.42 ± 0.015	1.02 ± 0.16
R4	c-$C_6H_{12} + OH$ (R11)	1.71 ± 0.040	1.14 ± 0.12
R4	$CH_3C_6H_5 + OH$ (R12)	2.08 ± 0.036	1.16 ± 0.30
R6	$C_3H_6 + Cl$ (R13)	0.63 ± 0.021	17.1 ± 2.2
R6	c-$C_6H_{12} + Cl$ (R14)	0.49 ± 0.014	16.1 ± 2.6
R6	$CH_3C_6H_5 + Cl$ (R15)	2.81 ± 0.043	16.7 ± 1.8
R7	$C_3H_6 + Cl$ (R13)	0.70 ± 0.014	18.9 ± 2.2
R7	c-$C_6H_{12} + Cl$ (R14)	0.55 ± 0.012	18.0 ± 2.8

Determinations of k_6 and k_7 at $T = 296 \pm 2$ K were carried out in a similar manner, with the exception of only two references being used to determine k_7 (C_3H_6 and c-C_6H_{12}) due to difficulties with overlapping peaks in $CH_3C_6H_5$ experiments. An exemplar relative rate plot for $k_{6,RR}(296 \pm 2$ K$)$ is shown in Figure 3. Weighted mean values from all such relative rate determinations were $k_{6,RR}(296 \pm 2$ K$) = (1.68 \pm 0.12) \times 10^{-10}$ cm^3 molecule^{-1} s^{-1} and $k_{7,RR}(296 \pm 2$ K$) = (1.85 \pm 0.18) \times 10^{-10}$

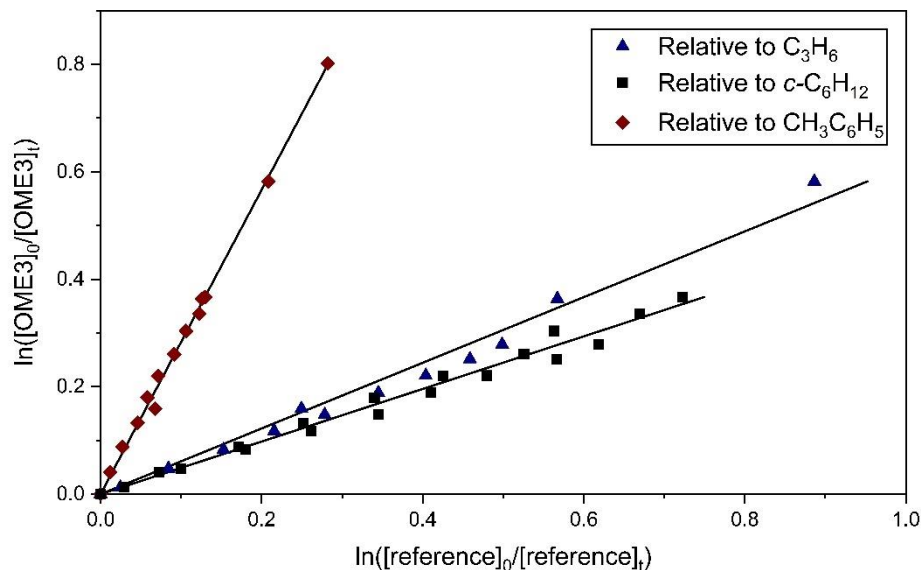205 cm^3 molecule^{-1} s^{-1}. The full set of plots and fits for k_{3-6} are available in the supplementary information (S2).

Figure 3: Representative plot, used to determine $k_{6RR}(296 \pm 2\ K)$ for Cl + OME3. Blue triangles correspond to use of C_3H_6 (R10) as reference; the black squares c-C_6H_{12} (R11) and the red diamonds $CH_3C_6H_5$ (R12). The solid lines are linear fits, the gradients of which were used to obtain k_6 (Eq.3) in conjunction with literature data (Table 1). Each experiment was repeated twice, and the resulting values of k_6 (Table 2) were averaged to obtain $k_6(296 \pm 2\ K) = (1.68 \pm 0.12) \times 10^{-10}\ cm^3\ molecule^{-1}\ s^{-1}$.

3.2 PLP-LIF determinations of $k_3(T)$
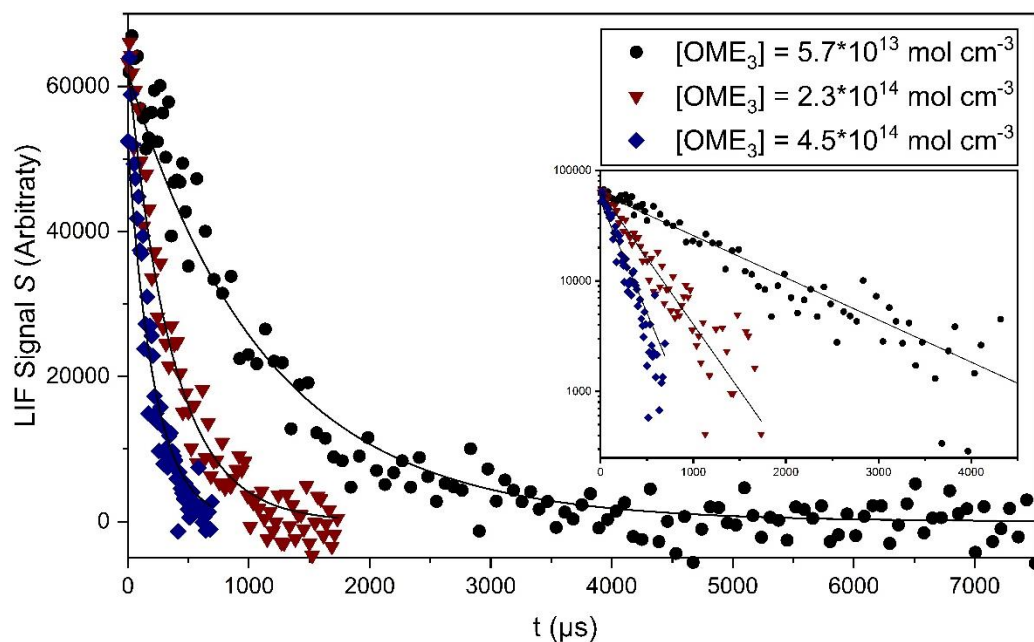
Figure 4: Displays OH decays obtained in PLP-LIF experiments at $T = 297$ K using three different [OME3]. Each was fit with Eq. (2) to determine pseudo first-order rate coefficients: $k_{obs} = (964 \pm 37)$ s^{-1} at [OME3] $= 5.7 \times 10^{13}$ molecule cm^{-3}; $k_{obs} = (2755 \pm 109)$ s^{-1} at [OME3] $= 2.3 \times 10^{14}$ molecule cm^{-3}; and $k_{obs} = (5252 \pm 220)$ s^{-1} at [OME3] $= 4.5 \times 10^{14}$ molecule cm^{-3}. Data are displayed on linear (main figure) and logarithmic (inset) y-axes.

PLP-LIF studies were carried under pseudo-first order conditions of [OME3] $\gg$ [OH] such that OH LIF time profiles, S(t), were described by a monoexponential decay expression (Eq. 2), following subtraction of measured baseline.

$$S(t) = S_0 e^{-k_{obs}t} \qquad (2)$$

S_0 describes the LIF signal at t = 0 in arbitrary units. It is proportional to the initial [OH] produced (R8) by the laser pulse. k_{obs} is the observed pseudo-first-order rate coefficient for OH decay, which includes components from both transport and reactive losses. Typical OH decay profiles are displayed in Figure 4, recorded in the presence of three different excess [OME3]. Other conditions ($P = 100$ mbar (N$_2$), $T = 297$ K, and [H$_2$O$_2$] $\approx 1 \times 10^{14}$ molecule cm^{-3}) were unchanged between experiments. OH LIF profiles were typically exponential over at least an order of magnitude and once fit to Eq. (2) yielded values of k_{obs} with high precision (standard errors were generally > 5%). Systematic errors from unintended radical side-reactions were considered unlikely given the following observation and checks: The low [OH] used ensured that OH losses by self-reaction or by reactions with the products of (R3) were minimal. Furthermore, aliphatic ethers do not have significant absorptions above 200 nm (Christianson et al., 2021), preventing the generation of organic radical fragments by the laser flash. Nevertheless, a series of experiments were performed in order to probe the impact of secondary chemistry. No systematic change in k_{obs} was obtained when the photolysis laser fluence was altered by a factor of three *via* modifications to the Q-switch delay. These observations suggest that any secondary chemistry had a negligible influence.
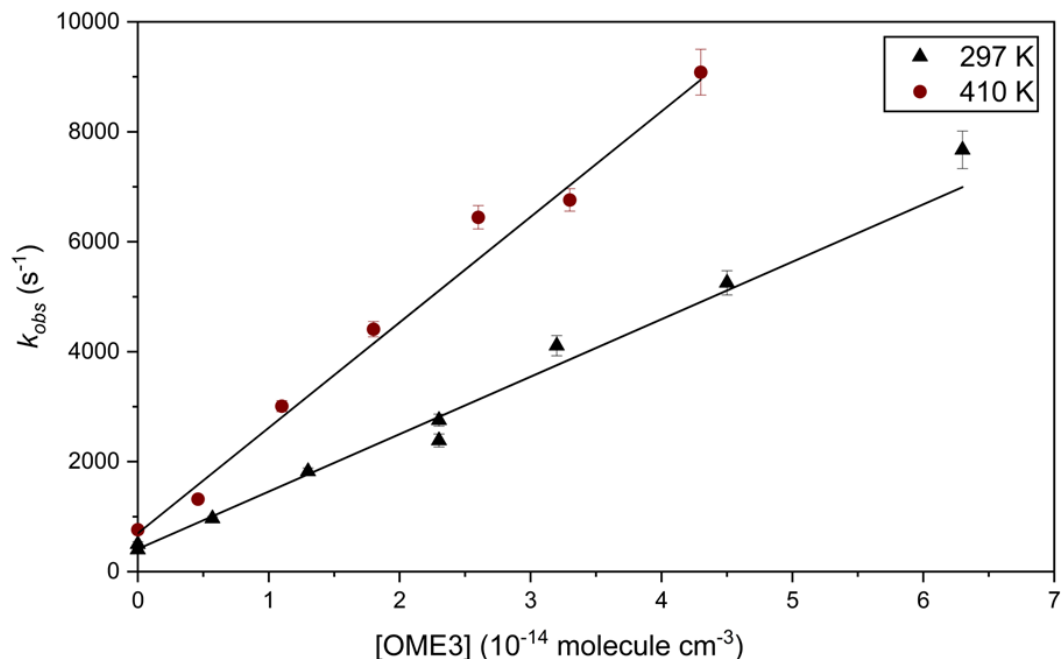
Figure 5: Representative bimolecular plot used to determine $k_3(T)$ from absolute PLP experiments. The black triangles depict results at ambient temperature, used to obtain k_3(297 K) = (1.05 ± 0.05) × 10⁻¹¹ cm³ molecule⁻¹ s⁻¹ *via* a weighted least squares linear fit of Eq. 3 to the data. The red circles similar depict data obtained at elevated temperature to yield k_3(410 K) = (1.92 ± 0.08) × 10⁻¹¹ cm³ molecule⁻¹ s⁻¹

Figure 5 displays a plot of k_{obs} vs. [OME-3] at $T = 297$ K; data were fit with Eq. (3) to obtain values of $k_3(T)$:

$$k_{obs} = k_3[OME3] + k_{loss} \quad (3)$$

where the term k_{loss} (in s⁻¹) corresponds to other losses of OH, in this case primarily the reaction of OH with the photolysis precursor H_2O_2 (R16) with small secondary contributions from diffusion and flow out of the reaction zone.

$$OH + H_2O_2 \rightarrow H_2O + HO_2 \qquad \qquad (R16)$$

When fitted linearly gradients correspond to $k_3(T)$ at each temperature and intercept values are in line with the predicted rate for (R16) with an estimated $[H_2O_2] = 10^{14}$ molecule cm⁻³ (around a few hundred s⁻¹). A mean of four values obtained at $T = (298 ± 2$ K) yielded $k_3 = (1.03 ± 0.13) × 10^{-11}$ cm³ molecule⁻¹ s⁻¹ in both N_2 and air regardless of pressure. An analogous series of experiments, conducted at elevated temperatures, were used to determine k_3(297 - 464 K). Details of conditions employed and results from all such PLP-LIF experiments are listed in Table 3.

Table 3: Absolute $k_3(T)$ determined *via* PLP-LIF in this work.

T / K	p / mbar	n^a	[OME3]^b	$k(T)^c$
297	78	16	1-37	1.05 ± 0.05
298	59	10	2-15	0.90 ± 0.06
300	56	8	2-18	0.96 ± 0.06
300	56	8	2-18	1.2 ± 0.2
337	76	8	2-25	1.00 ± 0.06
357	80	10	1-14	1.05 ± 0.04
373	74	8	1-12	1.21 ± 0.12
390	39	8	1-15	1.80 ± 0.09
410	33	13	1-14	1.92 ± 0.08
464	66	13	1-14	2.9 ± 0.2
469	33	13	1-14	2.3 ± 0.2

Notes: a n = number of B determinations, excluding those where [OME3] = 0; b = units of concentration were 10^{14} molecule cm⁻³; c = units of k were 10^{-11} cm³ molecule⁻³ s⁻³

Figure 6 represents all k3 results from this work in Arrhenius format. Whilst k_3(T) displayed approximately conventional Arrhenius behaviour at elevated temperatures, little change in the rate coefficient was observed between $T = 297$ K and $T = 390$ K. Potential explanations for this non-Arrhenius behaviour are explored in section 3.3 below, together with a comparison to results for similar oxygenated VOC + OH.
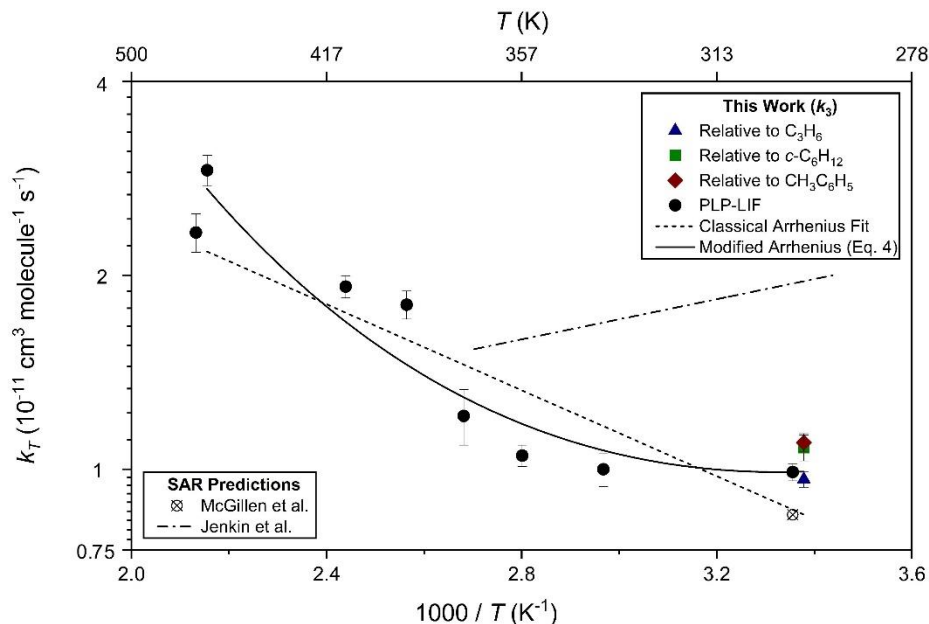
Figure 6: Arrhenius plot displaying $k_3(T)$ results from this work obtained *via* PLP–LIF and relative rate experiments. Displayed as the dotted line is the poor fit to the classical Arrhenius expression and the solid line the fit to the modified Arrhenius expression (equation 4); the dot-dash line depicts calculated $k_3(290–370 K)$ using the SAR proposed by Jenkin et al. (2018). Error bars are representative of measurement reproducibility only. These data are further discussed in section 3.3.

Experiments to determine accurate $k_4(T)$ in direct PLP-LIF experiments were not successful. Whilst reasonable exponential decays were recorded for the removal of OH in the presence of [OME4], nonlinearities were observed in the bimolecular plots of parameter k_{obs} vs. [OME4]. These observations were indicative of an inability to reliably saturate the gas flow through the bubbler with OME4, meaning that values of [OME4] calculated from manometric measurements were likely overestimates. Semi quantitative results were obtained in conditions when bubbler flows were smallest and the reaction cell was maintained at a slightly elevated temperature of $T = 340$ K. Here the bubbler was most likely to saturate with OME4 to allow for accurate concentration determination, and condensation of OME4 in the reactor was avoided. This data indicated that (R4) proceeds with a rate coefficient $k_4(340\ K) \approx 1 \times 10^{-11}$ cm^3 molecule^{-1} s^{-1}, in line with the ambient temperature relative rate determinations from this work.

3.3   Discussion of Kinetic Results

Determinations of $k_3(298 \pm 2\ K) = (1.03 \pm 0.13) \times 10^{-11}$ cm^3 molecule^{-1} s^{-1} (PLP-LIF) and $k_3(296 \pm 2\ K) = (1.04 \pm 0.09) \times 10^{-11}$ cm^3 molecule^{-1} s^{-1} (relative rate), between the different methods agree well with one another, especially when considering systematic uncertainties. These kinetic methods rely upon different critical assumptions (absolute knowledge of [OME-3] for

PLP-LIF, reference rate coefficients for relative-rate) and have complementary strengths and weaknesses, lending a high degree of confidence to these results. Nevertheless, when considering the systematic uncertainties inherent to these experiments (exact [OME] for the PLP-LIF determinations; the uncertainties in reference rate coefficient values for the relative rate experiments) we consider quoting a more conservative overall $k_3(297 \pm 3 \text{ K}) = (1.0 \pm 0.2) \times 10^{-11}$ cm^3 molecule^{-1} s^{-1} appropriate. Rate coefficients for (R4) were determined solely from relative rate experiments, giving an averaged value of $k_4(296 \pm 2 \text{ K}) = (1.11 \pm 0.10) \times 10^{-11}$ cm^3 molecule^{-1} s^{-1}. While complementary PLP-LIF experiments were not possible due to the limited volatility of OME4, semi-quantitative results indicate a rate coefficient $k_4(340 \text{ K}) \approx 1 \times 10^{-11}$ cm^3 molecule^{-1} s^{-1}, in support of the relative rate results. Given the increased uncertainty surrounding this value we recommend a value of $k_4(297 \pm 3 \text{ K}) = (1.1 \pm 0.4) \times 10^{-11}$ cm^3 molecule^{-1} s^{-1}. To the best of our knowledge, these results represent the first reported kinetic data for (R3-R4) under atmospherically relevant conditions.

In the absence of prior experimental studies of (R3- R4), it is difficult to meaningfully critique these values further. Table 4 presents a comparison of ambient temperature k-values for the reactions of OME and related compounds with OH. There is a clear trend whereby the larger compounds react with OH faster than those with fewer CH_2 groups, although this effect is lessened as the compounds become larger such that the difference between OME3 and OME4 is small-to-negligible. A similar sequential increase in reactivity has been reported upon successive addition of CH_2 groups by Mairean et al. (2024) for a series of seven *cis*-3-hexenyl esters. In this study the authors observed an increase of around 0.5×10^{-11} cm^3 molecule^{-1} s^{-1} per additional CH_2 group. Mellouki et al (1995) also reported such a trend for the OH-initiated oxidation of a series of ethers, although in their case the enhancement in reactivity from each additional CH_2 group was smaller. This was suggested to stem from the inductive effect of the ethereal oxygens. These trends are in line with the basic principle of SAR, whereby each additional oxidisable group contributes to additional reactivity, in this case starting from the well-studied molecule dimethyl ether (CH_3OCH_3), which is included in the training set of the Jenkin SAR. However, calculations based on an established SAR (Jenkin et al., 2018) appear to overpredict the reactivity of these molecules, for example $k_{3\text{Jenkin}}(298 \text{ K}) = 1.9 \times 10^{-11}$ cm^3 molecule^{-1} s^{-1}. This overprediction from the Jenkin SAR appears common to (R3) and (R4) and the available literature for OH + OME1 (Table 4). A similar overprediction was recently observed for OH + 2,2,5,5-tetramethyloxolane (TMO) (Mapelli et al., 2022). A lack of suitable literature data has likely limited progress on training SAR for OH + ether reactions. Rate coefficients for these reactions can also be estimated by an extension of the electrotopological approach which has proved an effective for estimating the reactivity of OH with alkanes and haloalkanes (McGillen et al., 2024). This method works by considering both the electronic state and connectivity of each atom in a molecule. This approach can be adapted to ethers by including a consideration for hydrogen-bonded pre-reaction complexes, a common feature of OH + oxygenate reactions, giving the values listed in Table 4 (Max McGillen, personal communication). This method proves more effective than the SAR from Jenkin et al. in terms of both absolute value and observed trends across the series.

Table 4: A comparison of predicted and experimental kinetic data for OH + OME and related compounds.

k / 10^{-11} cm^3 molecule^{-1} s^{-1}

OH +	Jenkin	McGillen	COSMO-RS	Experiment	Notes on experimental values
OME0 (dimethyl ether)	0.26	0.14	0.42	0.28	Recommended value from IUPAC evaluation with $\Delta \log k = 0.08$ (or $\sim 20\%$)(Atkinson et al., 2006). The absolute rate coefficient studies that form the basis of the preferred values (Arif et al., 1997; Bonard et al., 2002; Mellouki et al., 1995; Tully and Droege, 1987), are in good agreement with the other two absolute temperature-dependent studies (Perry et al., 1977; Wallington et al., 1988).
OME1	0.82	0.52	0.40	(0.44 ± 0.02) (0.46 ± 0.16) (0.55 ± 0.06) (0.50 ± 0.04) (0.49 ± 0.01) (0.49 ± 0.02)	(Bänsch and Olzmann, 2019) (Wallington et al., 1997), absolute (Wallington et al., 1997), relative to c-C_6H_{12} (Wallington et al., 1997), relative to ethylene (Porter et al., 1997), absolute (Thuner et al., 1999), relative to c-C_6H_{12}
OME2	1.38	0.70	0.42	-	Not reported to the best of our knowledge
OME3	1.94	0.85	0.44	(1.0 ± 0.2)	This work, (R3), PLP-LIF and RR
OME4	2.50	0.99	0.49	(1.1 ± 0.4)	This work, (R4), RR only

COSMO-RS was used to estimate values (Table 4) based on a combined DFT-parameterisation approach (Klamt, 1993, 1996, 2018). This method was able to estimate rate constants to a reasonable accuracy without the requirement for training on related structures, however it struggles to predict trends along the series from CH_3OCH_3. This could be due to extremely similar charge density surfaces across the series or due to deviation from the pre-reaction complex formation assumed for all oxygenates by the model. The proprietary nature of the software makes more thorough interpretation of these results challenging. Evidence for the likely participation of hydrogen-bonded complexes was provided by the results obtained with PLP-LIF for k_3 over the range of temperatures 294K to 464 K (Figure 6). Conventional Arrhenius-like behaviour was observed for $k_3(\geq 400$ K). The region of unchanging $k_3(297 - 390$ K) may be indicative of a change in mechanism across this temperature range. Hyrogen bonded pre-reaction complexes have previously been suggested to explain similar observations in the case of other OH + oxygenated VOC reactions. Such "U-shaped" Arrhenius plots have been observed for OH reactions with oxygenated VOC, notably dimethyl ether (Arif et al., 1997; Bonard et al., 2002; Mellouki et al., 1995), acetone (Wollenhaupt et al., 2000), methyl pivalate (Mapelli et al., 2023; Wallington et al., 2001), diethyl ether, a series of di-alkoxy methanes (Calvert et al., 2020) and most recently TMO (Mapelli et al., 2022). Experimental constraints meant we could not confirm these observations *via* the relative rate method, except at ambient temperature. We were able to achieve a

good fit to the modified Arrhenius expression Eq. (4) used by Rutto et al. to describe OH + cyclopentanone and derivatives (Rutto et al., 2024):

$$k(T) = A\left(\frac{T}{300}\right)^{\alpha} e^{\left(-\frac{E}{R}\left(\frac{1}{T}-\frac{1}{300}\right)\right)} \quad (4)$$

Where $A = (9.9 \pm 0.3) \times 10^{-12}$ cm^3 s^{-1}, $\alpha = (12.4 \pm 1.5)$ (dimensionless) and E/R = (-3717 ± 534) K. We note that, by analogy with the other reactions of OH with oxygenates noted in section 3.3 above, and as implied by Eq. 4, k_3 may increase at lower temperatures and that this k_3(297 K) value used here may be an underestimate of k_3 in cooler atmospheric conditions, e.g. the upper troposphere. It was not possible to investigate this more fully, given the lack of suitable low-temperature apparatus in York or Iasi. Also displayed on Fig. 4 are k_3(294 – 370 K) calculated using the Jenkin et al. SAR, which clearly over-predicts experimental k_3 values and exhibits more distinctive non-Arrhenius behaviour, and k_3(298 K) calculated using the SAR from McGillen.

Results from the OME + Cl   determinations were $k_{6,RR}$(296 $\pm$ 2 K) = $(1.68 \pm 0.12) \times 10^{-10}$ cm^3 molecule^{-1} s^{-1} and $k_{7,RR}$(296 $\pm$ 2 K) = $(1.85 \pm 0.18) \times 10^{-10}$ cm^3 molecule^{-1} s^{-1}. Given inherent uncertainties in reference rate coefficients used here, the lack of complementary PLP-LIF experimental data, or indeed any previous literature on we suggest conservative values of k_6(296 K) = $(1.7 \pm 0.4) \times 10^{-10}$ cm^3 molecule^{-1} s^{-1} and k_7(296 $\pm$ 2 K) = $(1.9 \pm 0.6) \times 10^{-10}$ cm^3 molecule^{-1} s^{-1} to more fully account for uncertainties. These rate coefficients are approximately an order of magnitude larger than the corresponding OME + OH values. Such enhanced reactivity towards Cl is not unusual for many classes of VOC, including ethers; reactions of Cl with THF (Alwe et al., 2013; Szymański and Sarzyński, 2020) and with dioxane (Giri et al., 2011; Li and Pirasteh, 2006) are similarly rapid. Alkanes react quickly with the chlorine radical, with their room-temperature reactivity increasing with the number of possible abstraction sites (in 10^{-10} cm^3 molecule^{-1} s^{-1}): $k(C_2H_6 + Cl) = 0.58 < k(C_3H_8 + Cl) = 1.4 < k(C_4H_{10} + Cl) + 2.05 < k(C_5H_{12} + Cl) = 2.7 < k(C_6H_{14} + Cl) = 3.3$ (McGillen et al., 2020). A similar trend can be observed for the OMEs ($\times 10^{-10}$ cm^3 molecule^{-1} s^{-1}): k(OME1 + Cl) = 1.4 (McGillen et al., 2020) $< k_6 = 1.67 < k_7 = 1.85$, suggesting a step size of around 1.5×10^{-10} cm^3 molecule^{-1} s^{-1}. It may be possible to infer by comparison that the reaction of OME2 with Cl would proceed with a rate coefficient around k(OME4 + Cl) 1.55×10^{-10} cm^3 molecule^{-1} s^{-1}, or at least in the range (1.40-1.67) $\times 10^{-10}$ cm^3 molecule^{-1} s^{-1}. Again, to the best of our knowledge, this work presents the first such determinations of k_6 and k_7.

4   Atmospheric Implications and Conclusions

Atmospheric lifetimes (τ) for OME3 and OME4 were estimated using Eq. 5, using [OH] = 1.13×10^6 molecule cm^{-3} representative of the troposphere (Lelieveld et al., 2016) in combination with rate coefficients from this work.

$$\tau = \frac{1}{k_{OH} \times [OH] + k_{Cl} \times [Cl]} \quad (5)$$

The resultant $\tau_3 \approx 24$ hours and $\tau_4 \approx 22$ hours may be overestimates for two reasons. Firstly, our ambient-temperature value may underestimate k_3 for conditions throughout the troposphere where temperatures below 297 K are common. Secondly,

the lifetime of OME may be constrained by (R6-7) with chlorine atoms in regions highly impacted by atmospheric chlorine.

350 Estimates for tropospheric [Cl] are subject to a high degree of spatial variability and vary widely, however using a large estimate of [Cl] = 1×10^4 molecule cm^{-3} (Li et al., 2018) and OME + Cl rate coefficients from this work, slightly shorter overall (OH and Cl reaction) lifetimes were estimated: $\tau_6 \approx$ 21 hours for OME3; $\tau_7 \approx$ 20 hours for OME4. Losses of OME to other atmospheric radicals, to O_3, and to photolysis are, to date, unreported and appear unlikely and as such we conclude that reactions (R3-4) are the dominant process for OME removal from the troposphere. Moriarty et al. (2003) used Eq. 5 to

355 estimate lifetimes, $\tau_1 \approx$ 25 hours and $\tau_2 \approx$ 16 hours, for the breakdown of dioxane and THF respectively. OME3 and OME4 have similar lifetimes to the solvents they may replace and so to better quantify their potential air quality impacts, Photochemical Ozone Creation Potential estimates ($POCP_E$) were calculated by the method reported by Jenkin et al. (2017). This parameter measures the extent of ozone generation, relative to an equivalent mass of ethene (CH_2CH_2), of a given VOC. $POCP_E$ were calculated from the structure of each compound, and the rate coefficient for reaction with OH. $POCP_E$ values

360 in of NW-European atmospheric conditions were estimated to be 26 (OME3) and 23 (OME4) by this method. Analogous estimates reveal significantly larger $POCP_E$ for dioxane and THF (40 and 55 respectively). These results suggest that OMEs would have a smaller negative impact on air quality than the traditional solvents they could replace. The rationale for this discrepancy is that, whilst OME have a similar reactivity to other traditional solvents, they are already more oxidised, with no C-C and fewer C-H bonds (per kg) available to provide fuel to atmospheric processes generating O_3 and NO_x.

365 To conclude, the application of two distinctive experimental approaches has revealed that OME3 and OME4 react with OH (R3 - R4) slower than predicted by the state-of-the-art SAR. A SAR currently-under-development from McGillen has proven more accurate when confronted with this structurally distinct class of compounds. These alternative solvents have similar atmospheric lifetimes yet appreciably smaller $POCP_E$ than the traditional, problematic solvents they could replace (THF and dioxane). These findings lend further strength to the growing case for OMEs as greener alternatives to THF and dioxane.

370 Further, results here represent a significant expansion to the extremely limited kinetic database for reactions of polyoxygenated VOC with OH. In the course of this work rate coefficients for both OMEs with atomic chlorine were determined, which are similar to THF and dioxane. These and similar results may allow for the training of improved SAR and similar predictive tools in future.

5   Data Availability

375 OME characterisation data (S1), Relative rate plots for k_{3-6} (S2), Gaussian Estimated Spectra (S3), COSMO-RS validation (S4), details of included files from computational procedures (S5a) and said files (S5b) are included in the supplement. Any further data are available upon request from the corresponding authors.

6 Author Contributions

Laser-based experiments were designed by TJD and conducted by TJD and CM. Chamber experiments were designed by TJD, IGB, CA and RIO and conducted by JDM, RKW and CR. Gaussian and COSMO-RS calculations were carried out by RKW and JDM respectively. The manuscript was written by TJD and JDM with assistance from other authors. TJD, IGB and CRM conceived of the overall project.

7 Competing Interests

The authors declare that they have no conflict of interest.

8 Acknowledgements

9 References

Alwe, H. D., Walawalkar, M., Sharma, A., Pushpa, K. K., Dhanya, S., and Naik, P. D.: Rate Coefficients for the Gas-Phase Reactions of Chlorine Atoms with Cyclic Ethers at 298 K, Int. J. Chem. Kinet., 45, 295–305, https://doi.org/10.1002/kin.20765, 2013.

Arif, M., Dellinger, B., and Taylor, P. H.: Rate Coefficients of Hydroxyl Radical Reaction with Dimethyl Ether and Methyl *tert* -Butyl Ether over an Extended Temperature Range, J. Phys. Chem. A, 101, 2436–2441, https://doi.org/10.1021/jp963119w, 1997.

Ariya, P.: Polar sunrise experiment 1995: hydrocarbon measurements and tropospheric Cl and Br-atoms chemistry, Atmos. Environ., 33, 931–938, https://doi.org/10.1016/S1352-2310(98)00254-4, 1999.

Ashcroft, C. P., Dunn, P. J., Hayler, J. D., and Wells, A. S.: Survey of Solvent Usage in Papers Published in *Organic Process Research & Development* 1997–2012, Org. Process Res. Dev., 19, 740–747, https://doi.org/10.1021/op500276u, 2015.

Atkinson, R. and Aschmann, S. M.: Kinetics of the gas phase reaction of Cl atoms with a series of organics at 296 ± 2 K and atmospheric pressure, Int. J. Chem. Kinet., 17, 33–41, https://doi.org/10.1002/kin.550170105, 1985.

410 Atkinson, R., Baulch, D. L., Cox, R. A., Crowley, J. N., Hampson, R. F., Hynes, R. G., Jenkin, M. E., Rossi, M. J., Troe, J., and IUPAC Subcommittee: Evaluated kinetic and photochemical data for atmospheric chemistry: Volume II – gas phase reactions of organic species, Atmospheric Chem. Phys., 6, 3625–4055, https://doi.org/10.5194/acp-6-3625-2006, 2006.

Bänsch, C. and Olzmann, M.: Reaction of dimethoxymethane with hydroxyl radicals: An experimental kinetic study at temperatures above 296 K and pressures of 2, 5, and 10 bar, Chem. Phys. Lett., 720, 19–24, https://doi.org/10.1016/j.cplett.2019.01.053, 2019.

415 Bloss, C., Wagner, V., Jenkin, M. E., Volkamer, R., Bloss, W. J., Lee, J. D., Heard, D. E., Wirtz, K., Martin-Reviejo, M., Rea, G., Wenger, J. C., and Pilling, M. J.: Development of a detailed chemical mechanism (MCMv3.1) for the atmospheric oxidation of aromatic hydrocarbons, Atmospheric Chem. Phys., 5, 641–664, https://doi.org/10.5194/acp-5-641-2005, 2005.

Bonard, A., Daële, V., Delfau, J.-L., and Vovelle, C.: Kinetics of OH Radical Reactions with Methane in the Temperature Range 295−660 K and with Dimethyl Ether and Methyl- tert -butyl Ether in the Temperature Range 295−618 K, J. Phys.
420 Chem. A, 106, 4384–4389, https://doi.org/10.1021/jp012425t, 2002.

Bryan, M. C., Dunn, P. J., Entwistle, D., Gallou, F., Koenig, S. G., Hayler, J. D., Hickey, M. R., Hughes, S., Kopach, M. E., Moine, G., Richardson, P., Roschangar, F., Steven, A., and Weiberth, F. J.: Key Green Chemistry research areas from a pharmaceutical manufacturers' perspective revisited, Green Chem., 20, 5082–5103, https://doi.org/10.1039/C8GC01276H, 2018.

425 Calvert, J. G., Orlando, J. J., Stockwell, W. R., and Wallington, T. J.: The Mechanisms of Reactions Influencing Atmospheric Ozone, Oxford University Press, https://doi.org/10.1093/oso/9780190233020.001.0001, 2015.

Calvert, J. G., Mellouki, A., Orlando, J. J., Pilling, M. J., and Wallington, T. J.: The mechanisms of atmospheric oxidation of the oxygenates, Oxford University Press, New York, 1 pp., https://doi.org/10.1093/oso/9780199767076.001.0001, 2020.

Christianson, M. G., Doner, A. C., Koritzke, A. L., Frandsen, K., and Rotavera, B.: Vacuum-ultraviolet absorption cross-
430 sections of functionalized cyclic hydrocarbons: Five-membered rings, J. Quant. Spectrosc. Radiat. Transf., 258, 107274, https://doi.org/10.1016/j.jqsrt.2020.107274, 2021.

Constable, D. J. C., Dunn, P. J., Hayler, J. D., Humphrey, G. R., Leazer, Jr., J. L., Linderman, R. J., Lorenz, K., Manley, J., Pearlman, B. A., Wells, A., Zaks, A., and Zhang, T. Y.: Key green chemistry research areas—a perspective from pharmaceutical manufacturers, Green Chem, 9, 411–420, https://doi.org/10.1039/B703488C, 2007.

435 Dagaut, Philippe., Liu, Renzhang., Wallington, T. J., and Kurylo, M. J.: Flash photolysis resonance fluorescence investigation of the gas-phase reactions of hydroxyl radicals with cyclic ethers, J. Phys. Chem., 94, 1881–1883, https://doi.org/10.1021/j100368a030, 1990.

de Gonzalo, G., Alcántara, A. R., and Domínguez de María, P.: Cyclopentyl Methyl Ether (CPME): A Versatile Eco-Friendly Solvent for Applications in Biotechnology and Biorefineries, ChemSusChem, 12, 2083–2097,
440 https://doi.org/10.1002/cssc.201900079, 2019.

Eckert, F. and Klamt, A.: COSMOtherm, Version C3. 0, Release 17.01, 2016.

European Environment Agency.: Air quality in Europe: 2020 report., Publications Office, LU, 2020.

Fenard, Y. and Vanhove, G.: A Mini-Review on the Advances in the Kinetic Understanding of the Combustion of Linear and Cyclic Oxymethylene Ethers, Energy Fuels, 35, 14325–14342, https://doi.org/10.1021/acs.energyfuels.1c01924, 2021.

445 Frisch, M. J., Trucks, G. W., Schlegel, H. B., Scuseria, G. E., Robb, M. A., Cheeseman, J. R., Scalmani, G., Barone, V., Petersson, G. A., Nakatsuji, H., Li, X., Caricato, M., Marenich, A. V., Bloino, J., Janesko, B. G., Gomperts, R., Mennucci, B., Hratchian, H. P., Ortiz, J. V., Izmaylov, A. F., Sonnenberg, J. L., Williams-Young, D., Ding, F., Lipparini, F., Egidi, F., Goings, J., Peng, B., Petrone, A., Henderson, T., Ranasinghe, D., Zakrzewski, V. G., Gao, J., Rega, N., Zheng, G., Liang, W., Hada, M., Ehara, M., Toyota, K., Fukada, R., Hasegawa, J., Ishida, M., Nakajima, T., Honda, Y., Kitao, O., Nakai, H.,
450 Vreven, T., Throssell, K., Montgomery, J. A., Peralta, J. E., Ogliaro, F., Bearpark, M. J., Heyd, J. J., Brothers, E. N., Kudin, K. N., Staroverov, V. N., Keith, T. A., Kobayashi, R., Normand, J., Raghavachari, K., Rendell, A. P., Burant, J. C., Iyengar, S. S., Tomasi, J., Cossi, M., Millam, J. M., Klene, M., Adamo, C., Cammi, R., Ochterski, J. W., Martin, R. L., Morokuma, K., Farkas, O., Foresman, J. B., and Fox, D. J.: Gaussian 16, 2016.

Giri, B. R., Roscoe, J. M., González-García, N., Olzmann, M., Lo, J. M. H., and Marriott, R. A.: Experimental and
455 Theoretical Investigation of the Kinetics of the Reaction of Atomic Chlorine with 1,4-Dioxane, J. Phys. Chem. A, 115, 5105–5111, https://doi.org/10.1021/jp201803g, 2011.

Hansen, D. A., Atkinson, R., and Pitts, J. N.: Rate constants for the reaction of hydroxyl radicals with a series of aromatic hydrocarbons, J. Phys. Chem., 79, 1763–1766, https://doi.org/10.1021/j100584a004, 1975.

Härtl, M., Gaukel, K., Pélerin, D., and Wachtmeister, G.: Oxymethylene Ether as Potentially CO2-neutral Fuel for Clean
460 Diesel Engines Part 1: Engine Testing, MTZ Worldw., 78, 52–59, https://doi.org/10.1007/s38313-016-0163-6, 2017.

Illés, Á., Rózsa, Z. B., Thangaraj, R., Décsiné Gombos, E., Dóbé, S., Giri, B. R., and Szőri, M.: An experimental and theoretical kinetic study of the reactions of hydroxyl radicals with tetrahydrofuran and two deuterated tetrahydrofurans, Chem. Phys. Lett., 776, 138698, https://doi.org/10.1016/j.cplett.2021.138698, 2021.

Jacob, E. and Maus, W.: Oxymethylene Ether as Potentially Carbon-neutral Fuel for Clean Diesel Engines Part 2:
465 Compliance with the Sustainability Requirement, MTZ Worldw., 78, 52–57, https://doi.org/10.1007/s38313-017-0002-4, 2017.

Jenkin, M. E., Derwent, R. G., and Wallington, T. J.: Photochemical ozone creation potentials for volatile organic compounds: Rationalization and estimation, Atmos. Environ., 163, 128–137, https://doi.org/10.1016/j.atmosenv.2017.05.024, 2017.

470 Jenkin, M. E., Valorso, R., Aumont, B., Rickard, A. R., and Wallington, T. J.: Estimation of rate coefficients and branching ratios for gas-phase reactions of OH with aliphatic organic compounds for use in automated mechanism construction, Atmospheric Chem. Phys., 18, 9297–9328, https://doi.org/10.5194/acp-18-9297-2018, 2018.

Jordan, A., Stoy, P., and Sneddon, H. F.: Chlorinated Solvents: Their Advantages, Disadvantages, and Alternatives in Organic and Medicinal Chemistry, Chem. Rev., 121, 1582–1622, https://doi.org/10.1021/acs.chemrev.0c00709, 2021.

475 Jordan, A., Hall, C. G. J., Thorp, L. R., and Sneddon, H. F.: Replacement of Less-Preferred Dipolar Aprotic and Ethereal Solvents in Synthetic Organic Chemistry with More Sustainable Alternatives, Chem. Rev., 122, 6749–6794, https://doi.org/10.1021/acs.chemrev.1c00672, 2022.

Klamt, A.: Estimation of gas-phase hydroxyl radical rate constants of organic compounds from molecular orbital calculations, Chemosphere, 26, 1273–1289, https://doi.org/10.1016/0045-6535(93)90181-4, 1993.

480   Klamt, A.: Estimation of gas-phase hydroxyl radical rate constants of oxygenated compounds based on molecular orbital calculations, Chemosphere, 32, 717–726, https://doi.org/10.1016/0045-6535(95)00352-5, 1996.

Klamt, A.: The COSMO and COSMO-RS solvation models, WIREs Comput. Mol. Sci., 8, e1338, https://doi.org/10.1002/wcms.1338, 2018.

Lelieveld, J., Gromov, S., Pozzer, A., and Taraborrelli, D.: Global tropospheric hydroxyl distribution, budget and reactivity,
485   Atmospheric Chem. Phys., 16, 12477–12493, https://doi.org/10.5194/acp-16-12477-2016, 2016.

Lelieveld, J., Klingmüller, K., Pozzer, A., Pöschl, U., Fnais, M., Daiber, A., and Münzel, T.: Cardiovascular disease burden from ambient air pollution in Europe reassessed using novel hazard ratio functions, Eur. Heart J., 40, 1590–1596, https://doi.org/10.1093/eurheartj/ehz135, 2019.

Lewis, A. C., Hopkins, J. R., Carslaw, D. C., Hamilton, J. F., Nelson, B. S., Stewart, G., Dernie, J., Passant, N., and
490   Murrells, T.: An increasing role for solvent emissions and implications for future measurements of volatile organic compounds, Philos. Trans. R. Soc. Math. Phys. Eng. Sci., 378, 20190328, https://doi.org/10.1098/rsta.2019.0328, 2020.

Li, M., Karu, E., Brenninkmeijer, C., Fischer, H., Lelieveld, J., and Williams, J.: Tropospheric OH and stratospheric OH and Cl concentrations determined from CH4, CH3Cl, and SF6 measurements, Npj Clim. Atmospheric Sci., 1, 29, https://doi.org/10.1038/s41612-018-0041-9, 2018.

495   Li, Z. and Pirasteh, A.: Kinetic study of the reactions of atomic chlorine with several volatile organic compounds at 240–340 K, Int. J. Chem. Kinet., 38, 386–398, https://doi.org/10.1002/kin.20171, 2006.

Mairean, C.-P., Roman, C., Arsene, C., Bejan, I.-G., and Olariu, R.-I.: Gas-Phase Kinetics of a Series of *cis* -3-Hexenyl Esters with OH Radicals under Simulated Atmospheric Conditions, J. Phys. Chem. A, 128, 6274–6285, https://doi.org/10.1021/acs.jpca.4c03069, 2024.

500   Mapelli, C., Schleicher, J. V., Hawtin, A., Rankine, C. D., Whiting, F. C., Byrne, F., McElroy, C. R., Roman, C., Arsene, C., Olariu, R. I., Bejan, I. G., and Dillon, T. J.: Atmospheric breakdown chemistry of the new "green" solvent 2,2,5,5-tetramethyloxolane via gas-phase reactions with OH and Cl radicals, Atmospheric Chem. Phys., 22, 14589–14602, https://doi.org/10.5194/acp-22-14589-2022, 2022.

Mapelli, C., Donnelly, J. K., Hogan, Ú. E., Rickard, A. R., Robinson, A. T., Byrne, F., McElroy, C. R., Curchod, B. F. E.,
505   Hollas, D., and Dillon, T. J.: Atmospheric oxidation of new "green" solvents – Part 2: methyl pivalate and pinacolone, Atmospheric Chem. Phys., 23, 7767–7779, https://doi.org/10.5194/acp-23-7767-2023, 2023.

Maurer, T., Hass, H., Barnes, I., and Becker, K. H.: Kinetic and Product Study of the Atmospheric Photooxidation of 1,4-Dioxane and Its Main Reaction Product Ethylene Glycol Diformate, J. Phys. Chem. A, 103, 5032–5039, https://doi.org/10.1021/jp990273k, 1999.

510   McGillen, M. R., Carter, W. P. L., Mellouki, A., Orlando, J. J., Picquet-Varrault, B., and Wallington, T. J.: Database for the kinetics of the gas-phase atmospheric reactions of organic compounds, Earth Syst. Sci. Data, 12, 1203–1216, https://doi.org/10.5194/essd-12-1203-2020, 2020.

McGillen, M. R., Michelat, L., Orlando, J. J., and Carter, W. P. L.: The use of the electrotopological state as a basis for predicting hydrogen abstraction rate coefficients: a proof of principle for the reactions of alkanes and haloalkanes with OH,
515   Environ. Sci. Atmospheres, 4, 18–34, https://doi.org/10.1039/D3EA00147D, 2024.

Mellouki, A., Teton, S., and Le Bras, G.: Kinetics of OH radical reactions with a series of ethers, Int. J. Chem. Kinet., 27, 791–805, https://doi.org/10.1002/kin.550270806, 1995.

Mellouki, A., Ammann, M., Cox, R. A., Crowley, J. N., Herrmann, H., Jenkin, M. E., McNeill, V. F., Troe, J., and Wallington, T. J.: Evaluated kinetic and photochemical data for atmospheric chemistry: volume VIII – gas-phase reactions of organic species with four, or more, carbon atoms ($\geq C_4$), Atmospheric Chem. Phys., 21, 4797–4808, https://doi.org/10.5194/acp-21-4797-2021, 2021.

Moriarty, J., Sidebottom, H., Wenger, J., Mellouki, A., and Le Bras, G.: Kinetic Studies on the Reactions of Hydroxyl Radicals with Cyclic Ethers and Aliphatic Diethers, J. Phys. Chem. A, 107, 1499–1505, https://doi.org/10.1021/jp021267i, 2003.

Perry, R. A., Atkinson, R., and Pitts, J. N.: Rate constants for the reaction of OH radicals with dimethyl ether and vinyl methyl ether over the temperature range 299–427 °K, J. Chem. Phys., 67, 611–614, https://doi.org/10.1063/1.434862, 1977.

Peter, A., Fehr, S. M., Dybbert, V., Himmel, D., Lindner, I., Jacob, E., Ouda, M., Schaadt, A., White, R. J., Scherer, H., and Krossing, I.: Towards a Sustainable Synthesis of Oxymethylene Dimethyl Ether by Homogeneous Catalysis and Uptake of Molecular Formaldehyde, Angew. Chem. Int. Ed., 57, 9461–9464, https://doi.org/10.1002/anie.201802247, 2018.

Porter, E., Wenger, J., Treacy, J., Sidebottom, H., Mellouki, A., Téton, S., and LeBras, G.: Kinetic Studies on the Reactions of Hydroxyl Radicals with Diethers and Hydroxyethers, J. Phys. Chem. A, 101, 5770–5775, https://doi.org/10.1021/jp971254i, 1997.

Prat, D., Wells, A., Hayler, J., Sneddon, H., McElroy, C. R., Abou-Shehada, S., and Dunn, P. J.: CHEM21 selection guide of classical- and less classical-solvents, Green Chem., 18, 288–296, https://doi.org/10.1039/C5GC01008J, 2016.

Ravishankara, A. R. and Davis, D. D.: Kinetic rate constants for the reaction of hydroxyl with methanol, ethanol, and tetrahydrofuran at 298 K, J. Phys. Chem., 82, 2852–2853, https://doi.org/10.1021/j100515a022, 1978.

Roman, C., Arsene, C., Bejan, I. G., and Olariu, R. I.: Investigations into the gas-phase photolysis and OH radical kinetics of nitrocatechols: implications of intramolecular interactions on their atmospheric behaviour, Atmospheric Chem. Phys., 22, 2203–2219, https://doi.org/10.5194/acp-22-2203-2022, 2022.

Rutto, P., Ubana, E., Selby, T. M., and Goulay, F.: Kinetic Study of OH Radical Reactions with Cyclopentenone Derivatives, J. Phys. Chem. A, 128, 8209–8219, https://doi.org/10.1021/acs.jpca.4c04060, 2024.

Saunders, S. M., Jenkin, M. E., Derwent, R. G., and Pilling, M. J.: Protocol for the development of the Master Chemical Mechanism, MCM v3 (Part A): tropospheric degradation of non-aromatic volatile organic compounds, Atmospheric Chem. Phys., 3, 161–180, https://doi.org/10.5194/acp-3-161-2003, 2003.

Schmitz, R., Russo, C., Ferraro, F., Apicella, B., Hasse, C., and Sirignano, M.: Effect of oxymethylene ether-2-3-4 (OME2-4) on soot particle formation and chemical features, Fuel, 324, 124617, https://doi.org/10.1016/j.fuel.2022.124617, 2022.

Seinfeld, J. H.: Atmospheric Chemistry and Physics: From Air Pollution to Climate Change, 1st ed., John Wiley & Sons, Incorporated, Newark, 1 pp., 2016.

Stuhr, M., Hesse, S., Faßheber, N., Wohler, M., Pal, M., Sakai, Y., Hemberger, P., and Friedrichs, G.: UV photolysis of oxalyl chloride: ClCO radical decomposition and direct Cl_2 formation pathways, Int. J. Chem. Kinet., 56, 482–498, https://doi.org/10.1002/kin.21723, 2024.

Sun, Z., Van Beers, H., Cuijpers, M., Somers, B., and Maes, N.: Design of experiments optimized OMEx-diesel blends on a heavy-duty engine − Part 1: Combustion and emissions analysis with EGR and injection timing variation, Fuel, 381, 133392, https://doi.org/10.1016/j.fuel.2024.133392, 2025.

555 Szymański, S. and Sarzyński, D. S.: Experimental study of the kinetics of reaction of chlorine atoms with tetrahydrofuran and fully deuterated tetrahydrofuran, Int. J. Chem. Kinet., 52, 957–963, https://doi.org/10.1002/kin.21413, 2020.

Thornton, J. A., Kercher, J. P., Riedel, T. P., Wagner, N. L., Cozic, J., Holloway, J. S., Dubé, W. P., Wolfe, G. M., Quinn, P. K., Middlebrook, A. M., Alexander, B., and Brown, S. S.: A large atomic chlorine source inferred from mid-continental reactive nitrogen chemistry, Nature, 464, 271–274, https://doi.org/10.1038/nature08905, 2010.

560 Thuner, L. P., Barnes, I., Maurer, T., Sauer, C. G., and Becker, K. H.: Kinetic study of the reaction of OH with a series of acetals at 298 ± 4 K, Int. J. Chem. Kinet., 31, 797–803, https://doi.org/10.1002/(SICI)1097-4601(1999)31:11<797::AID-JCK6>3.0.CO;2-C, 1999.

Tully, F. P. and Droege, A. T.: Kinetics of the reactions of the hydroxyl radical with dimethyl ether and diethyl ether, Int. J. Chem. Kinet., 19, 251–259, https://doi.org/10.1002/kin.550190308, 1987.

565 Wallington, T. J., Liu, R., Dagaut, P., and Kurylo, M. J.: The gas phase reactions of hydroxyl radicals with a series of aliphatic ethers over the temperature range 240–440 K, Int. J. Chem. Kinet., 20, 41–49, https://doi.org/10.1002/kin.550200106, 1988.

Wallington, T. J., Hurley, M. D., Ball, J. C., Straccia, A. M., Platz, J., Christensen, L. K., Sehested, J., and Nielsen, O. J.: Atmospheric Chemistry of Dimethoxymethane ($CH_3OCH_2OCH_3$): Kinetics and Mechanism of Its Reaction with OH
570 Radicals and Fate of the Alkoxy Radicals $CH_3OCHO(\bullet)OCH_3$ and $CH_3OCH_2OCH_2O(\bullet)$, J. Phys. Chem. A, 101, 5302–5308, https://doi.org/10.1021/jp9631184, 1997.

Wallington, T. J., Ninomiya, Y., Mashino, M., Kawasaki, M., Orkin, V. L., Huie, R. E., Kurylo, M. J., Carter, W. P. L., Luo, D., and Malkina, I. L.: Atmospheric Oxidation Mechanism of Methyl Pivalate, $(CH_3)_3CC(O)OCH_3$, J. Phys. Chem. A, 105, 7225–7235, https://doi.org/10.1021/jp010308s, 2001.

575 Winer, M., Lloyd, A. C., Darnall, K. R., Atkinson, R., and Pitts, J. N.: Rate constants for the reaction of OH radicals with n-propyl acetate, sec-butyl acetate, tetrahydrofuran and peroxyacetyl nitrate, Chem. Phys. Lett., 5, 1977.

Wollenhaupt, M., Carl, S. A., Horowitz, A., and Crowley, J. N.: Rate Coefficients for Reaction of OH with Acetone between 202 and 395 K, J. Phys. Chem. A, 104, 2695–2705, https://doi.org/10.1021/jp993738f, 2000.

Zhang, X., Kumar, A., Arnold, U., and Sauer, J.: Biomass-derived Oxymethylene Ethers as Diesel Additives: A
580 Thermodynamic Analysis, Energy Procedia, 61, 1921–1924, https://doi.org/10.1016/j.egypro.2014.12.242, 2014.

Zhao, S., Liang, H., Hu, X., Li, S., and Daasbjerg, K.: Challenges and Prospects in the Catalytic Conversion of Carbon Dioxide to Formaldehyde, Angew. Chem., 134, e202204008, https://doi.org/10.1002/ange.202204008, 2022.

Zhenova, A., Pellis, A., Milescu, R. A., McElroy, C. R., White, R. J., and Clark, J. H.: Solvent Applications of Short-Chain Oxymethylene Dimethyl Ether Oligomers, ACS Sustain. Chem. Eng., 7, 14834–14840,
585 https://doi.org/10.1021/acssuschemeng.9b02895, 2019.

Zhou, S., Barnes, I., Zhu, T., Bejan, I., and Benter, T.: Kinetic Study of the Gas-Phase Reactions of OH and NO_3 Radicals and O_3 with Selected Vinyl Ethers, J. Phys. Chem. A, 110, 7386–7392, https://doi.org/10.1021/jp061431s, 2006.